Bifurcation of the Subtropical South Equatorial Current against New Caledonia in December 2004 from a Hydrographic Inverse Box Model*

ALEXANDRE GANACHAUD+ AND LIONEL GOURDEAU

Institut de Recherche pour le Développement, Laboratoire d'Etudes en Géophysique et Océanographie Spatiales, UMR5566, IRD/CNES/CNRS/UPS, Nouméa, New Caledonia

WILLIAM KESSLER

Pacific Marine Environmental Laboratory/National Oceanographic and Atmospheric Administration, Seattle, Washington

(Manuscript received 20 August 2007, in final form 8 February 2008)

ABSTRACT

The South Equatorial Current (SEC), the westward branch of the South Pacific subtropical gyre, extends from the equator to 30°S at depth. Linear ocean dynamics predict that the SEC forms boundary currents on the eastern coasts of the South Pacific islands it encounters. Those currents would then detach at the northern and southern tips of the islands, and cross the Coral Sea in the form of jets. The Fiji Islands, the Vanuatu archipelago, and New Caledonia are the major topographic obstacles on the SEC pathway to the Australian coast. Large-scale numerical studies, as well as climatologies, suggest the formation of three jets in their lee: the north Vanuatu jet (NVJ), the north Caledonian jet (NCJ), and the south Caledonian jet (SCJ), implying a bifurcation against the east coast of each island. The flow observed during the SECALIS-2 cruise in December 2004 between Vanuatu and New Caledonia is presented herein. An inverse box model is used to provide quantitative transport estimates with uncertainties and to infer the pathways and boundary current formation. For that particular month, the 0–2000-m SEC inflow was found to be 20 ± 4 Sv (1 Sv ≡ 10^6 m^3 s^{-1}) between Vanuatu and New Caledonia. Of that, 6 ± 2 Sv bifurcated to the south in a boundary current against the New Caledonia coast (the Vauban Current), and the remainder exited north of New Caledonia, feeding the NCJ. The flow is comparable both above and below the thermocline, while complex topography, associated with oceanic eddy generation, introduces several recirculation features. To the north, the NCJ, which extends down to 1500 m, was fed not only by the SEC inflow, but also by waters coming from the north, which have possibly been recirculated. To the south, a westward current rounds the tip of New Caledonia. A numerical simulation suggests a partial continuity with the deep extension of the Vauban Current (this current would then be the SCJ) while the hydrographic sections are too distant to confirm such continuity.

1. Introduction

The subtropical part of the Pacific South Equatorial Current (SEC) carries thermocline waters toward the Australian coast. This water originates to the east, in the center of the subtropical gyre (Donguy 1994), and bifurcates at the coast of Australia, with a fraction feeding the East Australian Current system and the remainder flowing north to the Solomon Sea and eventually reaching the equator (Tsuchiya et al. 1989). This circulation pattern extends down to intermediate levels, as revealed by water mass properties and float trajectories (Qu and Lindstrom 2004; Davis 2005; Maes et al. 2007). However, the SEC splits upon encountering the major topographic obstacles of Fiji (180°E), the Vanuatu archipelago (~168°E), and New Caledonia (~165°E). Vanuatu and New Caledonia overlap meridionally to span a latitude width from 14°S to 23°S (Fig. 1a). (The reefs of New Caledonia extend to 18°S so that the bar-

* Joint Institute for the Study of the Atmosphere and Ocean Contribution Number 1459 and Pacific Marine Environmental Laboratory Contribution Number 3112.

+ Additional affiliation: Pacific Marine Environmental Laboratory/National Oceanographic and Atmospheric Administration, Joint Institute for the Study of the Atmosphere and Ocean, Seattle, Washington.

Corresponding author address: Alexandre Ganachaud, Institut de Recherche pour le Développement, BP A5 Noumea, New Caledonia. E-mail: alexandre.ganachaud@noumea.ird.nc

DOI: 10.1175/2008JPO3901.1

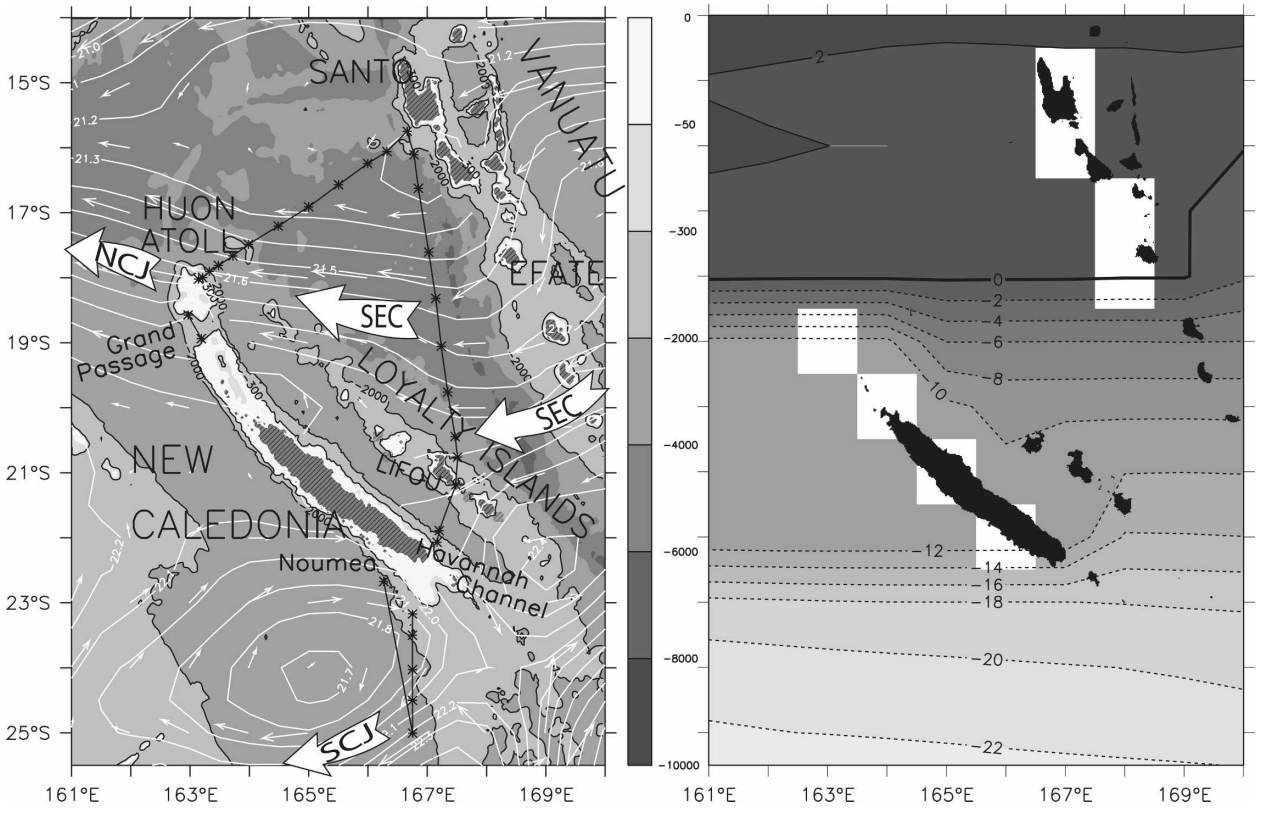

FIG. 1. (left) SECALIS-2 cruise: topography (m) and station position (stars). Land is hatched. Overlaid is the Montgomery potential and currents on $\sigma_\theta = 25$ m^2 s^{-2}, derived from the CARS climatology (Ridgway et al. 2002; Ridgway and Dunn 2003), along with the main currents described in the text (NCJ, SEC, and SCJ). (right) Island rule streamfunction, derived from the wind field (Sv). White squares show the topographic resolution from the CARS climatology data.

rier is about twice as long at the 50-m isobath as the island itself.) These two island groups form a broad channel about 500 km wide with the Loyalty Islands in between. Linear ocean dynamics require the incoming SEC waters to form boundary currents against the east side of islands or seamount ridges (Godfrey 1989), which then cross the Coral Sea zonally as narrow currents (Webb 2000). This "island rule" of Godfrey (1989) is a linear calculation that determines the net meridional wind-driven Sverdrup mass transport between an island and the coast to its east, including the western boundary transport along the east coast of the island (Wajsowicz 1993; Pedlosky et al. 1997). Figure 1b shows the island rule streamfunction as integrated from South America and then from island to island, including Australia (not in Fig. 1), based on the European Remote Sensing (ERS) satellite scatterometer winds. This calculation suggests a 10–11 Sv (1 Sv $\equiv 10^6$ m^3 s^{-1}) northwestward transport between New Caledonia and Vanuatu, with an important part of the flow occurring at the northern tip of New Caledonia. This linear calculation also requires that 6–7 Sv of the SEC inflow north of 23°S is deflected south and exits the area within a western boundary current becoming a jet to the west of New Caledonia as it detaches.

The jets, first identified in numerical models and climatologies (Webb 2000; Qu and Lindstrom 2002; Ridgway and Dunn 2003; Kessler and Gourdeau 2006), are the north Vanuatu jet (NVJ), centered at 13°S; the north Caledonia jet (NCJ; Fig. 1a), centered at 18°S; and the south Caledonia jet (SCJ; Fig. 1a), centered at 26°S. For convenience, we will define the SEC flow *exiting* the Vanuatu–New Caledonia region as being either northwestward or southward. While the broad-scale SEC inflow has been known since Wyrtki (1962a), its splitting and the existence of its jets is a more recent discovery. The NCJ has been observed for the first time at the northern extremity of the New Caledonia reef as a thin, intense flow extending in depth down to 1500 m (Gourdeau et al. 2008). The SCJ has been seen in models (Webb 2000) and climatologies (Ridgway and Dunn 2003, their Fig. 8a), but has never been measured near New Caledonia. How the SEC splits depend on the many ridges and channels within the archipelagoes. The

Commonwealth Scientific and Industrial Research Organisation (CSIRO) Atlas of Regional Seas (CARS) climatology provides an indication of the large-scale features, with about 10–12 Sv flowing northwest between New Caledonia and Vanuatu. (This transport estimate is based on a meridional calculation at 167°E, thereby avoiding most boundary current issues; but it is equivocal over short distances based on this climatology.) There have been two previous examinations of hydrographic sections in this region that have produced very different estimates of the transport (Sokolov and Rintoul 2000; Andrews and Clegg 1989). Neither is directly comparable to the present study, but the differences should be understood and will be discussed below.

The lack of knowledge of the amount of water transiting between New Caledonia and Vanuatu, and the suspected presence of boundary currents and bifurcation of the SEC against the eastern coast of New Caledonia motivated a series of hydrographic surveys between the two archipelagoes—the SECALIS cruises (Ganachaud et al. 2006; Gourdeau et al. 2008). The second SECALIS cruise (SECALIS-2) formed a closed box between Vanuatu and New Caledonia and another one south of New Caledonia. This cruise is analyzed here to describe how the large-scale flow interacts with the topographic features, and to give some insights on the pathways feeding the north and south New Caledonia jets. We calculate geostrophic and Ekman transports and adjust them with a hydrographic inverse box model (Wunsch 1996) so that conservation of mass and other quantities are ensured. The inverse model corrects the barotropic and Ekman components and a full error calculation allows a quantitative statement about the transport values and uncertainties to be made. The analysis is compared with a high-resolution ocean model simulation to provide a synoptic view of the circulation.

2. Data and inverse model

a. Hydrographic data

During the SECALIS-2 cruise, 30 CTD stations (Fig. 1) were collected between the surface and 1000–2000 m. The cruise track was designed to estimate the boundary currents and net (coast to coast) transports between New Caledonia and Vanuatu, forming a closed box with its two northern legs. On the southern leg along 166.7°E, most CTD stations reached only a depth of 1000 m for technical reasons, but two end-point stations (25°S, 166.7°E and 22.7°S, 166.2°E) reached 2000 m to allow calculation of the integral transport. Observations of temperature and salinity were made with an autonomous Sea-Bird CTD-19. The temperature and salinities had a respective resolution (precision) of 0.001°C (0.001°C) and 10^{-4} PSU (0.005 PSU), which is sufficient for our present application (Ganachaud et al. 2006). Currents in the first 250 m were recorded on a shipboard broadband 150-KHz ADCP. The cruise was conducted in December 2004, when seasonal analyses suggests that the SEC is close to its maximum value (Kessler and Gourdeau 2007; Morris et al. 1996), with a possible (although not detected in the Kessler and Gourdeau numerical model) impact on the NCJ. The trade winds were strong just before the cruise, but weak during the cruise.

In addition to the classical CTD treatment detailed in the cruise report (Ganachaud et al. 2006), temperature and salinity profiles were filtered using a 7-m median to remove spikes before integration on 20-m bins. This operation ensured static stability over the water column. Missing data in the first 60 db were extrapolated upward; missing data in the last 10 db were extrapolated downward. Geostrophic velocities in the vicinity of sloping topography ("bottom triangles") were calculated by horizontally extrapolating the next, deeper station pair density slope (see Ganachaud 2003 for a discussion). One station just south of the Santo, Vanuatu, deep tip (16.1°S, 166.8°E) was removed from the calculation as probably in error (see the discussion).

b. Inverse model

Geostrophic currents and transports between station pairs are calculated relative to a deep reference level, or the depth of the shallowest station along sloping bottom. Large mass imbalances are found between the sections based on this initial guess, and an inverse model is used to adjust the flow and estimate uncertainties on diagnostics. The following two distinct boxes are defined (Fig. 1a): a north box based on the Havannah–Santo–Huon, New Caledonia, trajectory, and a south box using the south meridional section at 166.7°E closed by the two 2000-m stations (see below). The basic inverse model technique follows that of Wunsch (1996) using a Gauss–Markov method to estimate reference-level velocities and Ekman transport along the hydrographic sections enclosing the domain so that the circulation satisfies basic conservation requirement (e.g., Ganachaud 2003). Mass (for both boxes), heat, and salt (for the north box) conservation constraints were applied over five isopycnal layers defined by potential density surfaces (Table 1). The Ekman transports across the sections were estimated by integration of the December 2004 Quick Scatterometer (QuikSCAT) average winds (information online at http://www.remss.com) and adjusted by the inverse model.

TABLE 1. Potential density surfaces used to constrain the inverse model; approximate corresponding waters masses; constraint on mass budget in the north box; dimensionless scaling factor applied to the heat and salt anomaly equations (NC = not constrained).

Upper (σ_θ, kg m^{-3})	Lower (σ_θ, kg m^{-3})	Water mass	Mass (Sv rms)	Heat scaling	Salt scaling
Surface	24	Tropical Surface Water	5	NC	0.1
24	26	Subtropical Lower Water	2	NC	0.1
26	27	Subantarctic Mode Water	1	0.5	0.1
27	27.5	Antarctic Intermediate Water	1	0.5	0.1
27.5	2000 m	Upper Circumpolar Deep Water	2	NC	NC
Surface	2000 m		5	NC	NC

Precipitation products (online at http://www.cdc.noaa.gov/cdc/data.cmap.html) provide a December 2004 estimate of 6 mm day^{-1} on average, which corresponds to a mass flux of 0.01 Sv over the north box, and much less for the south box. This is much smaller than mass residual uncertainties, and freshwater fluxes were not resolved.

A priori requirements on mass conservation were determined following the error estimates of Ganachaud (2003). Those are given in Table 1 for the north box. A larger allowance of ±2 Sv was attributed to the deepest layer to account for possible exchanges with the ocean below 2000 db. Anomaly equations are used to enforce heat (layer 3–4) and salt (layer 1–4) conservation with a weight inversely proportional to the mass conservation a priori error times the standard deviation of temperature or salinity variations within the respective layers, with a scaling factor. This scaling factor is determined experimentally so that all constraints are met and mass residuals are indistinguishable from zero within error bars (Table 1). Cross-isopycnal transfers are allowed within the box, within the range from $\pm 1 \times 10^{-4}$ cm s^{-1} at the bottom of layers 3–4 to $\pm 1 \times 10^{-3}$ cm s^{-1} at the bottom of layers 1–2. For the southern box, mass conservation solely was required as in Table 1, which is the constraint provided by the western section (made of the two 2000-m stations) that is an integral between 25°S and the New Caledonian reef. This configuration was used to take advantage of a deeper reference level between the two 2000-m stations.

For the northern box, the reference level was set at 2000 m, and initial reference velocities were chosen at 0 ± 1 cm s^{-1}, except in the following shallow waters near the shelf: 1) in the Grand Passage (0 ± 10 cm s^{-1}); 2) close to Huon (5.75 ± 5 cm s^{-1}); and 3) close to Havannah (10 ± 5 cm s^{-1} southeastward). Those shallow station pair reference velocities were chosen using surface ADCP velocities averaged over 150–206 m, below direct wind influence. Overall in the north box, and using such initial reference velocities on the sides, shipboard ADCP (S-ADCP) and geostrophic velocities averaged over three stations agree within 2–7 cm s^{-1}. Away from the boundaries, initial uncertainties (or the range of adjustment) on deep reference velocities were taken at 1 cm s^{-1} and increased according to vertical shear near the reference level. Those are close to the final ones (see Fig. 4) because the information gained through the inversion (i.e., the reduction of uncertainties) is on the large scales. Within the inverse model formulation of either Wunsch (1996) or Ganachaud (2003), this would mean that only the off-diagonal elements of the error covariance matrix are significantly modified. For the southern box, the initial reference velocities were taken at 0 ± 5 cm s^{-1} along the meridional section (1000-m reference level) and 0 ± 1 cm s^{-1} for the western section (2000-m reference level) because of the deeper level and larger station spacing.

A solution to the reference level velocities, the Ekman transports, and the advective and diffusive vertical transfers between layers within the box must be found so that all constraints (13 for the north box and 5 for the south box) are met. The initial Ekman transports required little change for overall balance, with final estimates at 0.3 ± 0.5 Sv northward (Huon–Santo), 0.7 ± 0.5 Sv westward (Havannah–Santo), and 0.1 ± 0.5 Sv westward across the south meridional section.

3. Results

a. Water masses

Water masses are identified by two prominent features in temperature and salinity (Fig. 2). Our analysis follows Wyrtki (1962b) and Sokolov and Rintoul (2000). Salinities attain a maximum near $\sigma_\theta = 25$ ($\theta \sim 21$°C) marking the South Pacific Tropical Water [(SPTW), see Qu and Lindstrom (2002); also called Subtropical Lower Water (SLW) by Wyrtki (1962b)] of eastern origins (Donguy 1994; Yeager and Large 2004; Johnson 2006). The salinity maximum occurs near 200 m in both sections in the north box (Figs. 3a,b) while it extends to the surface south of 22°S (Fig. 3c), consistent with the CARS climatology (Ridgway and Dunn 2003). This outcrop was noted on the World Ocean Circulation Experiment (WOCE) 155°E section by Sokolov

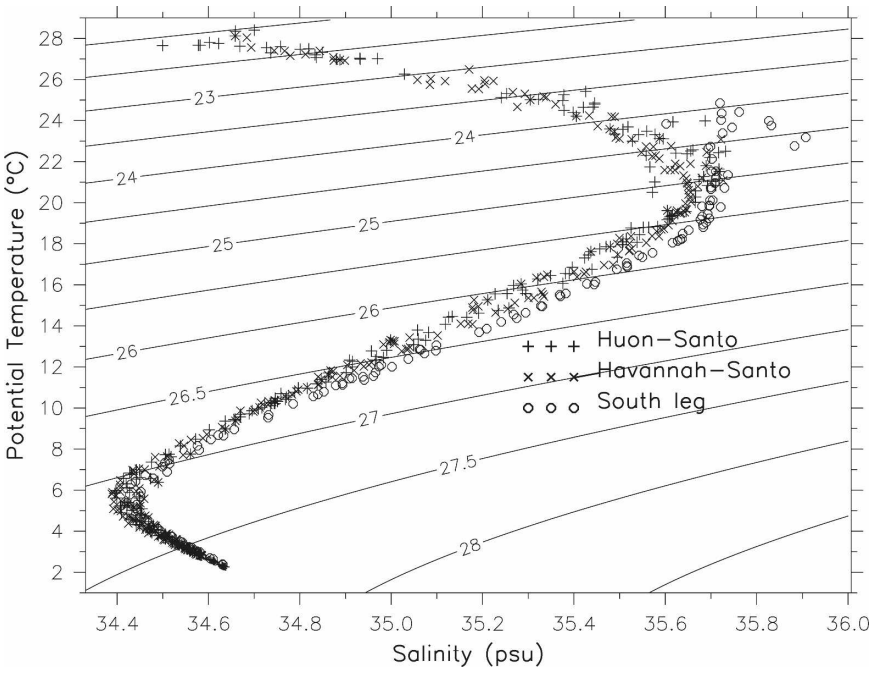

FIG. 2. Potential temperature–salinity relation during the SECALIS-2 cruise. Each symbol is assigned to a specific leg.

and Rintoul (2000) as being the boundary between the SPTW, with warm and salty characteristics of central/east Pacific origins (Donguy 1994), and Subtropical Mode Water (STMW; $\theta = 14°$–$20°$C), emanating from the north part of the Tasman Sea (Donguy and Hénin 1977; Roemmich and Cornuelle 1992; Roemmich et al. 2005; Tsubouchi et al. 2007; Holbrook and Maharaj 2008). Near 167°E, this distinction coincides with the southern tip of New Caledonia, as suggested by the south boundary of the maximum salinity tongue (Sokolov and Rintoul 2000, their Fig. 4). North of 22°S, both water masses are brought from the east by the SEC (Sokolov and Rintoul 2000). For our transport calculations, SPTW and STMW are grouped in a single layer, Wyrtki's "SLW," which encompasses the salinity maximum between $\sigma_\theta = 24$ and $\sigma_\theta = 26$ (Fig. 2).

North of 22°S, the SPTW is capped by Tropical Surface Water (TSW) above $\sigma_\theta = 24$, with warm temperatures (25°–28°C) and low salinities (34.5–35.3) associated with high precipitation in the South Pacific convergence zone (Donguy 1987, 1994).

Near 600 m, waters in the density range close to $\sigma_\theta = 27$ ($\theta \sim 8°$C) were identified as the Subantarctic Mode Water (SAMW) by McCartney (1977). SAMW forms by deep convection on the northern edge of the Antarctic Circumpolar Current and is advected northward into the South Pacific subtropical gyre. Climatological water properties suggest that the Vanuatu–New Caledonia SAMW comes from the southeast Pacific and is carried by the SEC [see Sokolov and Rintoul (2000) for a thorough discussion]. In our inverse model, we use a broad layer between $\sigma_\theta = 26$ and $\sigma_\theta = 27$ that comprises the SAMW waters.

Near $\sigma_\theta = 27.2$ ($\theta \sim 5.5°$C), a pronounced salinity minimum identifies the Antarctic Intermediate Water (AAIW) that is created by subduction in the South Pacific polar front (50°–60°S). AAIW of southeastern origins invades the Coral and Tasman Seas through a north branch that flows between New Caledonia and Vanuatu and a south branch that flows south of New Caledonia (Wyrtki 1962b; Tsuchiya 1991; Sokolov and Rintoul 2000). At 20°S, the AAIW salinity minimum is most pronounced (Fig. 3a) between 700 and 900 m, and is 100 m shallower on the north section, following the density horizon (Fig. 3b). The salinity minimum is enhanced against the coast of New Caledonia in both sections (Figs. 3a,b), as well as in the south section at 23.5°S (Fig. 3c).

Between $\sigma_\theta = 27.5$ (~1300 m) and our maximum depth of 2000 m lies the "oxygen minimum waters," described by Wyrtki (1962b) as the transition between the AAIW and the Coral Sea Circumpolar Deep Water (CDW). The CDW is formed in the Southern Ocean and is identified as a weak salinity maximum ($S = 34.73$, $\theta \sim 1.6°$C) near 2800 m in the Tasman Sea (Wyrtki 1962b; Sokolov and Rintoul 2000). The Coral

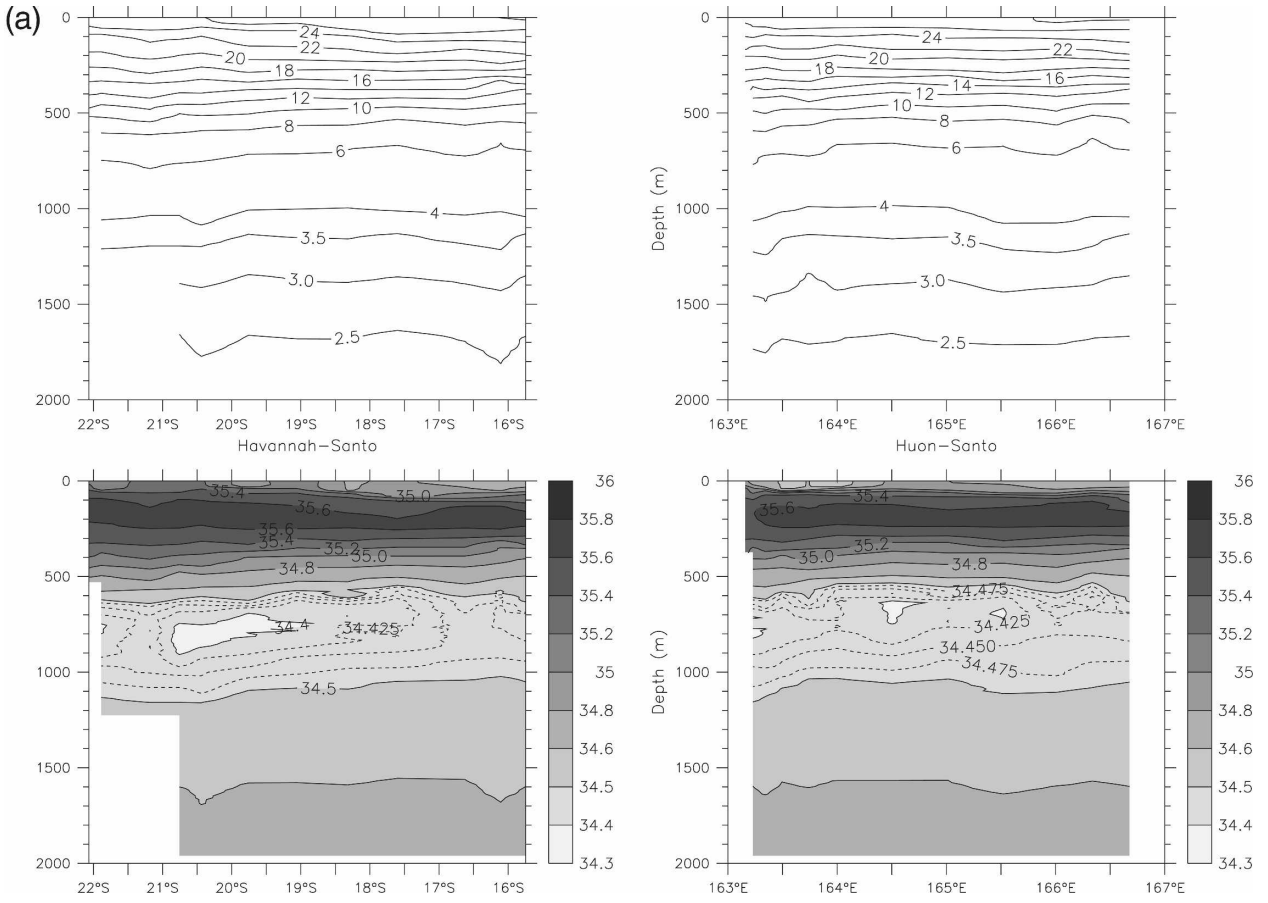

FIG. 3. Potential temperature and salinity sections along (a) the east leg (left; Havannah–Santo) and the north leg (right; Huon–Santo) and (b) the south leg.

Sea, however, is an enclosed basin isolated from these waters below the sill depth of the Cato Trough near Australia (23°S, 155°E) at about 2800 m so that the salinity is homogeneous below that depth in the Coral Sea. Wyrtki described these oxygen minimum waters as advecting slowly from the north of the Solomon Sea and filling the Coral Sea. We labeled the layer between $\sigma_\theta = 27.5$ and 2000 m, a mixture of CDW and AAIW, as the "upper Circumpolar Deep Water," bearing in mind that its origins are not entirely clear.

Because the upper waters (SLW and TSW) are of different relevance in the large-scale context than the lower waters (SAMW, AAIW, and upper CDW), we separately diagnose the transports above and below $\sigma_\theta = 26$.

b. *Transports in the northern box*

The SECALIS-2 velocity field through the Havannah–Santo section displays a southeastward boundary current against the east coast of New Caledonia near 22°S, transporting 3.8 ± 0.4 Sv above $\sigma_\theta = 26$ (Fig. 4a, third panel), which has been called the Vauban Current by Hénin et al. (1984). This current extends below $\sigma_\theta = 26$, carrying an extra 1.8 Sv (Fig. 4a, lower panel) for a total of 5.7 ± 2 Sv. The transport is to the southeast at all depths, with the SLW contributing most (Table 2, second column, "Havannah–Lifou"). North of the Loyalty Ridge, the flow is broad and to the west (positive on Fig. 4a; the section is meridional on that leg), corresponding to the SEC inflow into the box, which was found to be 7.8 ± 0.6 Sv above $\sigma_\theta = 26$ and 12.6 ± 3 Sv below, the horizontally integrated flow being westward in all layers. This inflow is split into two streams—a broad one south of 18°S and a narrow one against Santo (Fig. 4a, lower two panels). The total inflow above 2000 m between Havannah and Santo, including Ekman transport, is 14 ± 3.6 Sv.

On the Huon–Santo section (Fig. 4b, upper two panels), a strong northwestward current is found against the east coast of New Caledonia and is conveniently identified as part of the NCJ (Webb 2000) although it is still, at this latitude, a boundary current. The NCJ is

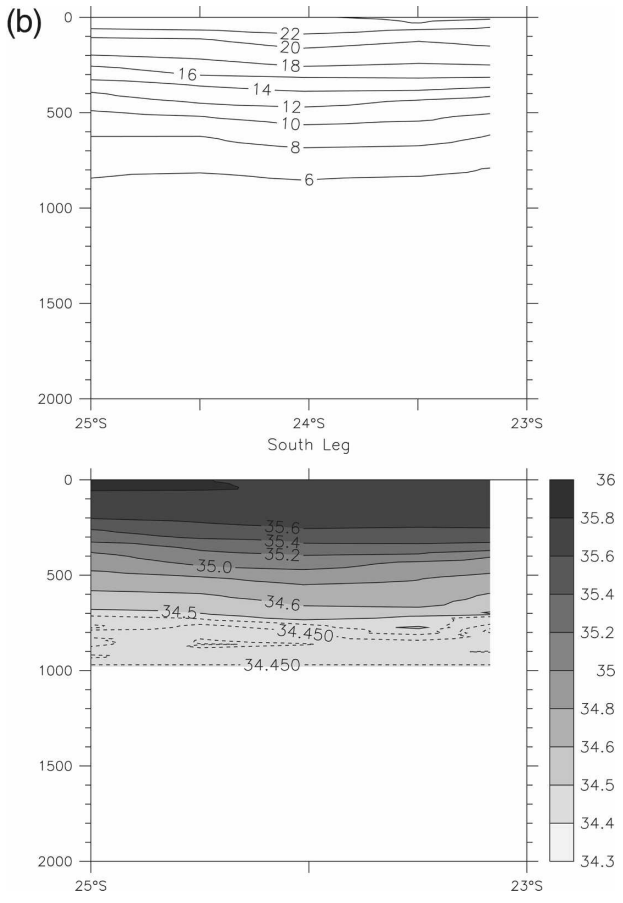

FIG. 3. (*Continued*)

composed of two cores—one against the coast and a secondary, broader one centered about 100 km offshore, aligned with the Loyalty Ridge (164.3°E). The upper NCJ transport is 6.7 ± 0.4 Sv (Fig. 4b, panel 3). It is flanked to its east by a broad southward countercurrent in the middle of the section (164.5°–166°E) and another northwestward current against Santo; each of these currents transport about 12 Sv, but in opposite directions so that the total cancels out (Fig. 4b, lower two panels). Across this section, the net transports are northward for all water masses (Table 2).

The net transport above 2000 m through the Huon–Santo section is close to that of the Havannah–Santo one, with 14.4 ± 3.6 Sv (5.7 ± 0.5 Sv above $\sigma_\theta = 26$), as expected through the mass conservation requirement. The transport in the narrow Grand Passage between the Huon Atoll and the northern New Caledonia reef (500 m deep × 30 km wide; Fig. 1) is explicitly calculated as part of the inversion, based on the two stations taken on its edges (Fig. 1); however, it is weak and below the estimated uncertainties (0.16 ± 1.8 Sv eastward). Because a strong westward current is commonly observed there by sailors, we made a sensitivity test by requiring an a priori westward ageostrophic transport of 5 ± 3 Sv spread over depth according to the more recent ADCP measurements of Gourdeau et al. (2008). The inverse model corrected the Grand Passage reference velocity and ageostrophic transports to cancel this a priori estimate, reflecting the fact that such large transport in the Grand Passage would go against our conservation requirement. We conclude that in December 2004, the flow through the Havannah–Santo and Huon–Santo sections did not require a strong Grand Passage transport at the present level of uncertainty.

c. Transports across the southern section

The adjusted velocities in the section south of New Caledonia (Fig. 1a) show a strong westward flow against the coast and an eastward flow south of 24°S (Fig. 4c, upper two panels). The S-ADCP data (not shown) suggest weaker velocities than the geostrophic ones in the 150–200-m range in both extremities of the section. The origin of this difference (10–15 cm s^{-1}) is not understood. It may be attributed to transient ageostrophic processes related with the sudden drop in the trade winds episode preceding the cruise or to tides or internal wave aliasing. The westward flow against the coast may correspond to the SCJ (see the discussion below), carrying 3.4 ± 1 Sv above $\sigma_\theta = 26$ (Fig. 4c, panel 4) for a total of 6 ± 3 Sv above 1000 m. The eastward flow to its south (5.7 ± 0.8 Sv above $\sigma_\theta = 26$ for a total of 8.6 ± 3 Sv) may be the northern part of the South Subtropical Countercurrent (STCC; Merle et al. 1969; Kessler and Gourdeau 2007).

4. Discussion: SEC pathways in December 2004

The estimated SECALIS-2 transports through our inverse box model are summarized in Fig. 5. To illustrate the large-scale circulation context, we refer to the 2004 yearly mean, vertically integrated transport of the OCCAM simulation at 1/12° (information online at http://www.noc.soton.ac.uk/JRD/OCCAM/). This configuration is documented in Lee et al. (2007). The model includes a mixed layer, and its vertical resolution ranges from 5 m to the surface to 200 m at depth with a total of 66 levels. The topography resolution is at 2 min. This numerical model shows how and where the SEC bifurcates against New Caledonia, after splitting against Fiji (180°W) and Vanuatu (Fig. 6).

a. Thermocline transports, north box

The thermocline waters (white arrows on Fig. 5, defined as flowing above $\sigma_\theta = 26$) give a 7.8 ± 0.6 Sv SEC

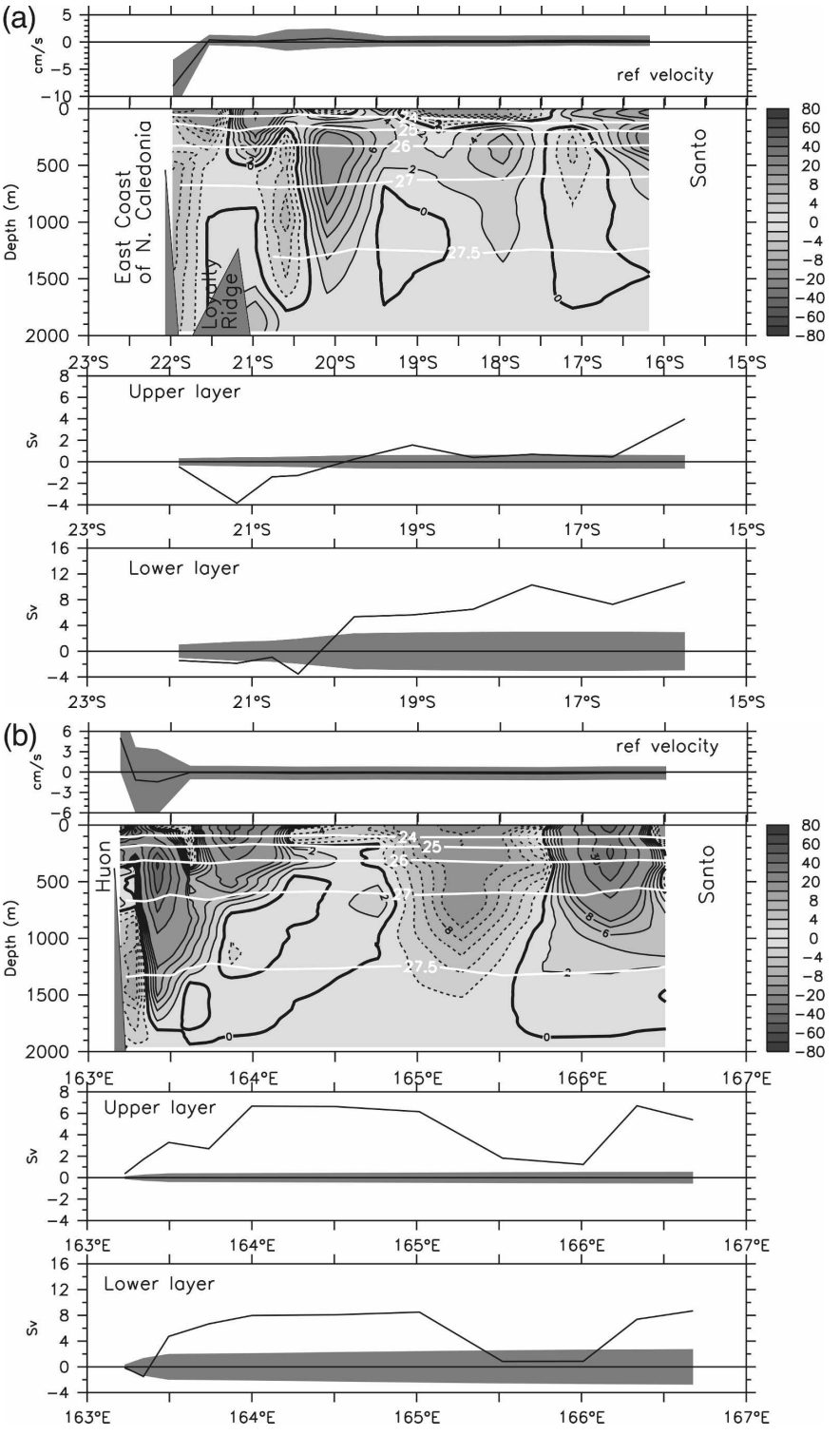

FIG. 4. (a) Havannah–Santo and (b) Huon–Santo sections. The top two panels give the estimated reference velocity (line) with uncertainties (shaded area, one standard deviation) and absolute velocity field for the SECALIS-2 cruise. Positive is (a) westward (northwestward as one approaches 22°S) and (b) northward; σ_θ surfaces are overlaid. The two lower panels indicate the cumulative transports from (a) south and (b) north for the upper (surface to $\sigma_\theta = 26$) and lower (down to 2000 m) layers (1std dev uncertainty shaded). (c) South section (positive westward; transport cumulative from south).

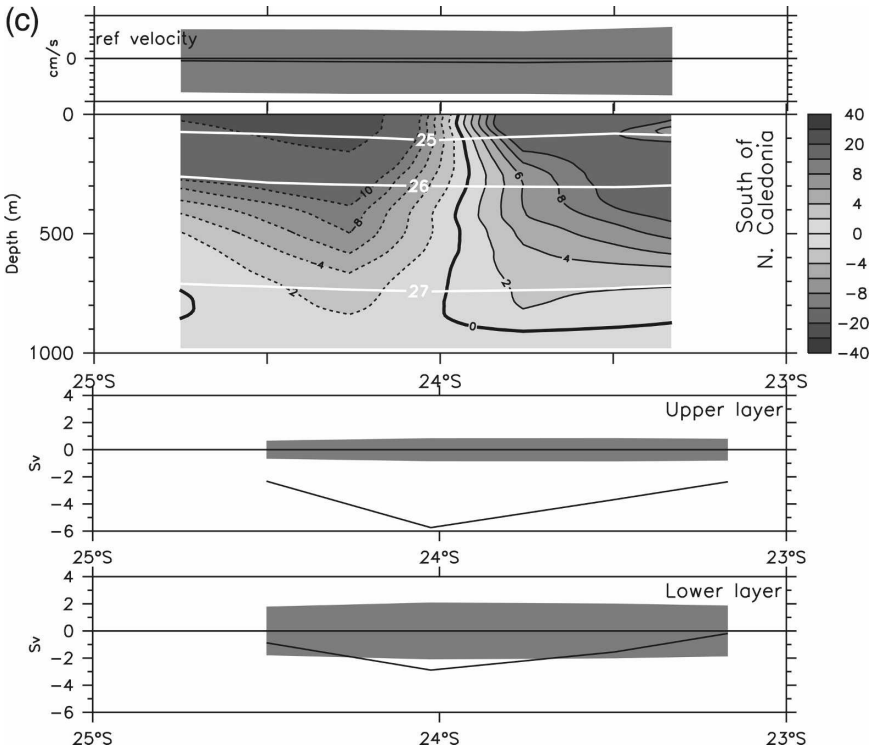

FIG. 4. (*Continued*)

inflow into the area (8.5, if one includes the Ekman transport), of which 4 ± 0.4 Sv turns south and exits south of the Loyalty Islands in the Vauban Current. This latter estimate may be an extreme, as suggested by a series of unpublished 0–250-m S-ADCP sections between New Caledonia and the Loyalty Islands (G. Eldin 2007, personal communication). The OCCAM simulation shows a weak Vauban Current, with most of the southward flow occurring east of the Loyalty Islands (Fig. 6). About 4 Sv of the SEC inflow occurs against the coast of Santo within a horizontal salinity maximum (Fig. 3b). The upper 265-m pathway in a global ocean general circulation model (OCCAM; not shown, but similar to the 0–2000 flow of Fig. 6) suggests a quasi-direct flow east of the Loyalty Islands ridge, connecting the SEC inflow and the NCJ as observed along the SECALIS-2 sections. The net thermocline water transport in the Vanuatu–New Caledonia channel is of 4.7 ± 0.6 Sv northwestward, including Ekman. It exits to the north partly in the NCJ and partly near Santo. (Mass cannot be exactly conserved between the two sections because of unavoidable residual noise and round-off errors on Fig. 5.) For that same density range, Sokolov and Rintoul (2000, their Fig. 16) inferred a much larger transport (16 Sv). Kessler and Gourdeau (2007) pointed out that such an enhanced SEC might have been a lagged response to the 1991/92 El Niño. However, the Sokolov and Rintoul (2000) estimate was based on transports calculation along a hydrographic section much farther west (155°E) and extrapolated to our region (165°E) based on climatological water mass properties. While the transport along 155°E is well de-

TABLE 2. Transports by water masses (Sv). Positive is northward (Havannah–Lifou and Huon–Santo); northwestward (Lifou–Santo). Ekman transport not included; uncertainties are one standard deviation. The transports do not sum up exactly as small imbalances are accommodated by cross isopycnal transfers and residual noise.

Water mass	Havannah–Lifou	Lifou–Santo	Huon–Santo
Tropical Surface Water	−1.2 ± 0.1	0.9 ± 0.2	0.7 ± 0.2
Subtropical Lower Water	−2.7 ± 0.3	7 ± 0.5	4.7 ± 0.4
Subantarctic Mode Water	−1 ± 0.4	6.5 ± 0.6	5.3 ± 0.5
Antarctic Intermediate Water	−0.7 ± 0.7	4.1 ± 1.2	3.9 ± 1.1
Upper Circumpolar Deep Water	−0.2 ± 0.4	2.1 ± 1.3	−0.5 ± 1.1

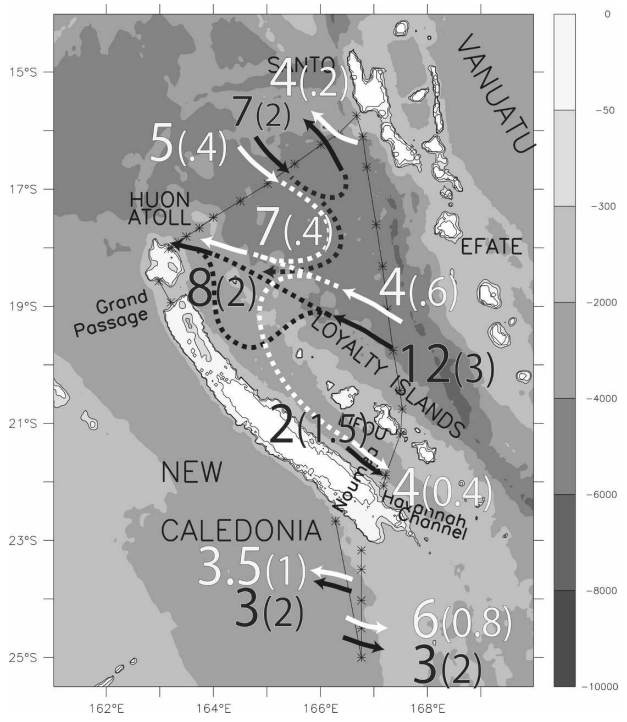

FIG. 5. SECALIS-2-estimated transports across selected sections (Sv), with Ekman transport excluded. The white numbers and arrows refer to transports above $\sigma_\theta = 26$, and the dark ones between $\sigma_\theta = 26$ and 2000 m (northern box, north of 22°S) or $\sigma_\theta = 27.75$ (approximately 1000 m; lower box, south of 22°S). The uncertainty (1 std dev) is given in the parenthesis.

termined, its partition between the different channels to the east is uncertain, because much of it occurs in narrow boundary currents that are neither resolved nor interpretable in large-scale water mass properties. The other existing estimate for the total transports in this channel comes from Andrews and Clegg (1989) who found no clear NCJ—a possible sampling issue (the authors had to extrapolate many profiles using a projection on normal modes, and the consequences on boundary current transport estimates is not clear).

b. Deep layers, north box

Below the thermocline (dark arrows on Fig. 5), the circulation patterns are similar. Dotted pathways were drawn based on cross section transport continuity, and pathways taken by Argo floats (Maes et al. 2007). The net deep SEC inflow is large (12.6 ± 3.1) with only 2 ± 1.5 Sv exiting south in the deep component of the Vauban Current. Most of the SEC inflow feeds the NCJ whose velocity field core extends deeper than 1500 m, consistent with the finding of Gourdeau et al. (2008) north of New Caledonia.

Because half of the deep part of the Vauban Current occurs in the first station pair below the last common depth of the two stations near the Havannah Channel (544 m), it results from the sum of horizontally linearly extrapolated density values and the additional barotropic adjustment by the inverse model. To test the robustness of this current, an experiment was done where the flow below 544 m was set to zero between these two stations. After adjustment by the inverse model, this configuration resulted in a 0.8 ± 1.2 Sv southward current occurring over the next station pair to the east, a lower value that is still consistent within uncertainties with the 2 ± 1.5 Sv. We therefore kept the "extrapolated" solution as our most realistic candidate, with 2 ± 1.5 Sv. The net deep northward flow is 2 Sv less in the north section than in the south section, which is allowed in the inversion because of residual uncertainties resulting from measurement noise of unresolved flow against the island shelves.

During the SECALIS cruise, a CTD station was made against the deep topographic protuberance below 700 m, south of Santo (16.1°S, 166.8°E; Fig. 1a). Including this station in the geostrophic calculation implied a strong westward flow (6 Sv, 30 cm s^{-1}) just against the protuberance, with a counterflow south of it. Such strong current is highly unlikely because the Vanuatu Ridge is closed at these depths, and we have no dynamical explanation for such current against an eastern boundary, so we excluded the 16.1°S station as a probable alias of the unresolved high-frequency signals. The northernmost station (15.75°S, 166.7°E) was used as the endpoint of both Huon–Vanuatu and Havannah–Santo sections in either case, so that the exclusion of the suspect profile did not change the coast-to-coast integrated transports, because those depend only on end stations.

A meridional CTD section north of the Huon Atoll, corroborated by a glider survey along the same track, estimated the NCJ transport at 10 Sv along 163°E in July 2005, but between the surface and 600 m (Gourdeau et al. 2008), similar to that of SECALIS-2 (11.4 ± 1 Sv). These close estimates may be fortuitous because of time variability and the fact that the Gourdeau et al. estimate may have included a northern-origin component in the NCJ, as suggested by numerical models (e.g., Figure 6) and Argo floats (Maes et al. 2007). While the NCJ was observed by Gourdeau et al. as a single core at 163°E, its upstream component estimated from SECALIS-2 is made of two cores—one against the Huon Atoll and the other one about 50 km to the east (Fig. 4b), possibly in the lee of the Loyalty Ridge.

c. Net flow, north box

Of the 20 ± 4 Sv SEC transport between the surface and 2000 dbar crossing the meridional section south of

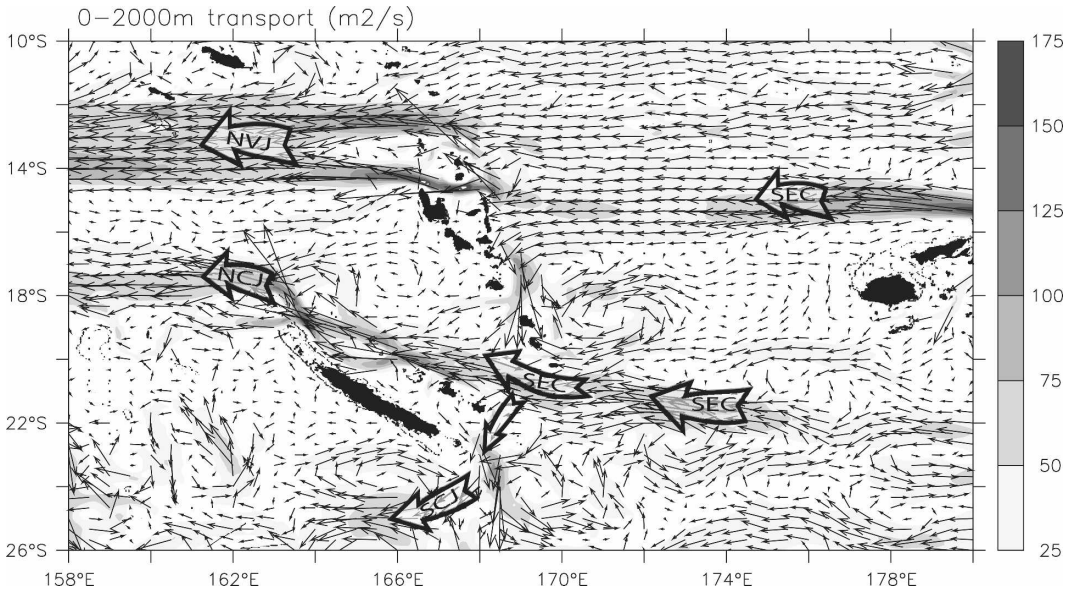

FIG. 6. Integrated transports between 0 and 2000 m from the annual 2004 average OCCAM simulation at 1/12°. The arrows give the direction of the transport; the shading its magnitude ($m^2\ s^{-2}$).

Vanuatu, 14 ± 3Sv exits the channel northwestward, while 6 ± 2 Sv turns south in the Vauban Current. This circulation is generally consistent with the CARS climatology (Fig. 1), with a broad westward inflow across 167.6°E between 22° and 16°S (see also Ridgway and Dunn 2003, Fig. 8f). CARS climatology suggests a net westward flow between New Caledonia and Vanuatu that is slightly smaller than ours, with 10–12 Sv. The CARS climatology estimate is similar to that of the Island Rule (Fig. 1b), which also predicts a Vauban Current/SCJ transport at about 6 Sv, as we found herein. The net inflow is by far smaller than the Sokolov and Rintoul (2000) extrapolation at 41 Sv, perhaps for the same reasons as discussed in section 4a above.

d. Bifurcation

The upper- and lower-layer transports in Fig. 5 both imply a bifurcation of the incoming SEC waters within the box. The time-averaged OCCAM transports over 1 yr (Fig. 6) show a relatively clear illustration of this bifurcation occurring near 20°–21°S. Examination of OCCAM snapshots and corresponding altimetric observation (J. Sudre 2007, LEGOS, personal communication) shows that at any given time, the eddy field combined with the presence of the Loyalty Islands and the Grand Passage blurs this picture and shows convoluted SEC pathways, which can be at all depths, with several branches that are likely sensitive to the numerous topographic features. Sensitivity experiments based on regional model simulation show that the bifurcation is highly dependant on the model configuration and may occur both east and west of the Loyalty ridge (Couvelard et al. 2008).

e. South box

A westward flow against the southern tip of New Caledonia is measured directly for the first time. A similar but weaker boundary current was observed south of the Fiji Islands (Stanton et al. 2001), upstream of the SEC. Such flow is implied by the "island rule" dynamics discussed above, and the CARS climatology shows such a westward flow down to the bottom, just south of New Caledonia, between 23° and 25°S (Fig. 1; and Ridgway and Dunn 2003, their Fig. 8f). This CARS climatology current resulted from interpolation of CTD data scattered in time and space there (Ridgway and Dunn 2003, their Fig. 2). In the CARS climatology this boundary current is flanked by a shallow (0–500 m) eastward current corresponding to the STCC, south of 25°S. A similar current is observed south of 24°S during SECALIS-2, but with a deeper extent.

f. SCJ

The island rule, CARS and numerical simulations (Webb 2000) suggest continuity between the southward branch of the SEC (the deeper part of the Vauban Current) and the westward flow against the southern tip of New Caledonia. Such continuity is not possible for confirmation from SECALIS-2, but OCCAM (Fig.

6) suggests that part of the south-bifurcated waters effectively take this SCJ route while 5–6 Sv recirculates eastward. In the deep layers, the SECALIS-2 data show an AAIW salinity minimum against New Caledonia (Fig. 2c), while the thermocline salinity maximum outcrops. This minimum is consistent with the hypothesis of continuity with the lower Vauban Current, while not proving it.

5. Conclusions

The SECALIS-2 cruise provides a first snapshot of the circulation and transports in the broad channel between New Caledonia and Vanuatu, as well as a description of the hypothesized, but previously unobserved, current structures south of New Caledonia. The use of an inverse box model allows for quantitative estimates of velocities, transports, and uncertainties. The SECALIS-2 results permits a description of the water pathways above and below the thermocline, with the broad, westward SEC splitting into branches as it encounters the numerous topographic features of the region.

Figure 5 provides a summary of the estimated transports. In December 2004, the net westward SEC flow between New Caledonia and Vanuatu was 20 ± 4 Sv, of which 6 ± 4 Sv bifurcated south, consistent with linear ocean dynamics (the "island rule") and numerical model analyses. The remainder, 14 ± 4 Sv, exited to the north between New Caledonia and Vanuatu, partially within a northward boundary current against the east coast of New Caledonia, and partially against the west coast of Santo Island. A bifurcation of the SEC waters is implied, as can be seen near 20°S in high-resolution numerical simulations. Numerical simulations also suggest that part of the southward flow against New Caledonia veers clockwise and rounds the southern tip of New Caledonia to form the South Caledonian Jet (SCJ), in agreement with the island rule. The SECALIS-2 observations show such an important westward flow just south of New Caledonia, consistent with a SCJ, but cannot distinguish it from temporary eddy flows. The snapshot has its inherent limitations, and the next development of this work will be the analysis of variations of the circulation with time, based on all four SECALIS cruises and the few other existing CTD profiles in the area. As Argo profiles accumulate, they will provide a fuller picture of the SEC, but the large transports occurring in narrow boundary currents will continue to require direct surveys such as the SECALIS cruises.

Acknowledgments. The SECALIS-2 cruise was supported by IRD and LEGOS, as exploratory experiments that contributed to the development of coordinated research in the southwest Pacific Ocean (Ganachaud et al. 2007). We are particularly grateful to the R/V *Alis* crew and the US25 (IRD) staff who made the SECALIS-2 cruise possible. E. Kestenare (IRD) processed the CTD and ADCP data. C. Maes (IRD) and two anonymous reviewers provided stimulating comments to improve the manuscript. J. Lefevre's (IRD) help with model analysis was appreciated. K. Ridgway kindly provided the CARS climatology data used on Fig. 1. AG thanks NOAA's Pacific Marine Environmental Laboratory and its director, Dr. Eddie Bernard, for hosting him during this work. This publication is partially funded by the Joint Institute for the Study of the Atmosphere and Ocean (JISAO) under NOAA Cooperative Agreement NA17RJ1232.

REFERENCES

Andrews, J. C., and S. Clegg, 1989: Coral Sea circulation and transport deducted from modal information models. *Deep-Sea Res.,* **36,** 957–974.

Couvelard, X., P. Marchesiello, L. Gourdeau, and J. Lefevre, 2008: Barotropic zonal jets induced by islands in the southwest Pacific. *J. Phys.Oceanogr.,* **38,** 2185–2204.

Davis, R. E., 2005: Intermediate-depth circulation of the Indian and South Pacific Oceans measured by autonomous floats. *J. Phys. Oceanogr.,* **35,** 683–707.

Donguy, J. R., 1987: Recent advances in the knowledge of the climatic variations in the tropical Pacific. *Prog. Oceanogr.,* **19,** 49–85.

——, 1994: Surface and subsurface salinity in the tropical Pacific Ocean: Relation with climate. *Prog. Oceanogr.,* **34,** 45–78.

——, and C. Hénin, 1977: Origin of the surface tropical water in the Coral and Tasman Seas. *J. Mar. Freshwater Res.,* **28,** 321–332.

Ganachaud, A., 2003: Error budget of inverse box models: The North Atlantic. *J. Atmos. Oceanic Technol.,* **20,** 1641–1655.

——, and Coauthors, 2006: SECALIS-2 cruise report, 4–18 December 2004. Centre IRD de Nouméa Rapports de Missions Sciences de la Mer No. 19, 80 pp.

——, and Coauthors, 2007: Southwest Pacific Ocean Circulation and Climate Experiment (SPICE)—Part I. Scientific background. CLIVAR Publication Series No. 111, NOAA/OAR Special Report, 37 pp.

Godfrey, J. S., 1989: A Sverdrup model of the depth-integrated flow for the world ocean allowing for island circulations. *Geophys. Astrophys. Fluid Dyn.,* **45,** 89–112.

Gourdeau, L., E. Kestenare, A. Ganachaud, J.-Y. Panche, L. Jamet, A. diMatteo, J. Verron, and X. Couvela, 2007: SECALIS-3 cruise report onboard R/V *ALIS,* 11–24 July 2005, 22°S–9°55S, 160°07E–168°10E. IRD, Sciences de la Mer: Océanographie Physique, Rapports de Mission No. 21, 80 pp.

——, W. S. Kessler, R. E. Davis, J. Sherman, C. Maes, and E. Kestenare, 2008: Zonal jets entering the Coral Sea. *J. Phys. Oceanogr.,* **38,** 715–725.

Hénin, C., J.-M. Guillerm, and L. Chabert, 1984: Circulation superficielle autour de la Nouvelle-Calédonie. *Océanogr. Trop.,* **19,** 113–126.

Holbrook, N. J., and A. M. Maharaj, 2008: Southwest Pacific Sub-

tropical Mode Water: A climatology. *Progr. Oceanogr.,* **77,** 298–315.

Johnson, G., 2006: Generation and initial evolution of a mode water θ–S anomaly. *J. Phys. Oceanogr.,* **36,** 739–751.

Kessler, W. S., and L. Gourdeau, 2006: Wind-driven zonal jets in the South Pacific Ocean. *Geophys. Res. Lett.,* **33,** L03608, doi:10.1029/2005GL025084.

——, and ——, 2007: The annual cycle of circulation of the southwest subtropical Pacific, analyzed in an ocean GCM. *J. Phys. Oceanogr.,* **37,** 1610–1627.

Lee, M.-M., A. J. George Nurser, A. C. Coward, and B. A. de Cuevas, 2007: Eddy advective and diffusive transports of heat and salt in the Southern Ocean. *J. Phys. Oceanogr.,* **37,** 1376–1393.

Maes, C., L. Gourdeau, X. Couvelard, and A. Ganachaud, 2007: What are the origins of the Antarctic Intermediate Waters transported by the North Caledonian Jet? *Geophys. Res. Lett.,* **34,** L21608, doi:10.1029/2007GL031546.

McCartney, M. S., 1977: Subantarctic Mode Waters. *A Voyage of Discovery, George Deacon 70th Anniversary Volume,* M. Angel, Ed., Pergamon, 103–119.

Merle, J., H. Rotschi, and B. Voituriez, 1969: Zonal circulation in the tropical western South Pacific at 170°E. *Bull. Japan Soc. Fish. Oceanogr.,* 91–98.

Morris, M., D. Roemmich, and B. Cornuelle, 1996: Observation of variability in the south Pacific subtropical gyre. *J. Phys. Oceanogr.,* **26,** 2359–2380.

Pedlosky, J., L. Pratt, M. Spall, and K. Helfrich, 1997: Circulation around islands and ridges. *J. Mar. Res.,* **55,** 1199–1251.

Qu, T., and E. Lindstrom, 2002: A climatological interpretation of the circulation in the western south Pacific. *J. Phys. Oceanogr.,* **32,** 2492–2508.

——, and ——, 2004: Northward intrusion of Antarctic Intermediate water in the western Pacific. *J. Phys. Oceanogr.,* **34,** 2104–2118.

Ridgway, K. R., and J. R. Dunn, 2003: Mesoscale structure of the East Australian Current System and its relationship with topography. *Prog. Oceanogr.,* **56,** 189–222.

——, ——, and J. L. Wilkins, 2002: Ocean interpolation by weighted least squares—Application to the waters around Australia. *J. Atmos. Oceanic Technol.,* **19,** 1357–1375.

Roemmich, D., and B. Cornuelle, 1992: The subtropical mode waters of the South Pacific Ocean. *J. Phys. Oceanogr.,* **22,** 1178–1187.

——, J. Gilson, J. Willis, P. Sutton, and K. Ridgway, 2005: Closing the time-varying mass and heat budgets for large ocean areas: The Tasman Box. *J. Climate,* **18,** 2330–2343.

Sokolov, S., and S. Rintoul, 2000: Circulation and water masses of the southwest Pacific: WOCE section P11, Papua New Guinea to Tasmania. *J. Mar. Res.,* **58,** 223–268.

Stanton, B., D. Roemmich, and M. Kosro, 2001: A shallow zonal jet south of Fiji. *J. Phys. Oceanogr.,* **31,** 3127–3130.

Tsubouchi, T., T. Suga, and K. Hanawa, 2007: Three types of South Pacific subtropical mode waters: Their relation to the large-scale circulation of the south Pacific subtropical gyre and their temporal variability. *J. Phys. Oceanogr.,* **37,** 2478–2490.

Tsuchiya, M., 1991: Flow path of the Antarctic intermediate Water in the western equatorial South Pacific Ocean. *Deep-Sea Res.,* **38** (Suppl.), 273–279.

——, R. Lukas, R. A. Fine, E. Firing, and E. Lindstrom, 1989: Source waters of the Pacific Equatorial Undercurrent. *Prog. Oceanogr.,* **23,** 101–147.

Wajsowicz, R. C., 1993: The circulation of the depth integrated flow around an island with application to the Indonesian throughflow. *J. Phys. Oceanogr.,* **23,** 1470–1484.

Webb, D., 2000: Evidence for shallow zonal jets in the South Equatorial Current region of the southwest Pacific. *J. Phys. Oceanogr.,* **30,** 706–720.

Wunsch, C., 1996: *The Ocean Circulation Inverse Problem*. Cambridge University Press, 437 pp.

Wyrtki, K., 1962a: Geopotential topographies and associated circulation in the Western South Pacific Ocean. *Aust. J. Mar. Freshwater Res.,* **13,** 89–105.

——, 1962b: The subsurface water masses in the western South Pacific Ocean. *Aust. J. Mar. Freshwater Res.,* **13,** 18–47.

Yeager, S. G., and W. G. Large, 2004: Late-winter generation of spiciness on subducted isopycnals. *J. Phys. Oceanogr.,* **34,** 1528–1547.